JMEPEG (2004) 13:226-231
DOI: 10.1361/10599490418442

1059-9495/$19.00

Proposed Modification to the Zheng and Hirt Fatigue Model

B.K.C. Yuen and F. Taheri

(Submitted 28 October 2003; in revised form 12 January 2004)

The Zheng and Hirt model describes the fatigue behavior of metals based on the tensile properties, thus eliminating the need for extensive fatigue crack propagation tests as required by other fatigue models. The model uses the fracture strength of the material based on a relationship. The predictability of the model was improved by incorporating into the equations the measured fracture strength of the material instead of the calculated value. An experimental investigation, consisting of both tension and fatigue testing on the 350WT category 5 steel, was performed to verify the proposed modification. The results showed that the modified model predicted the fatigue crack growth rates of the steel with a greater accuracy than the original model.

Keywords 350WT steel, fatigue crack propagation, fracture strength, tensile properties, Zheng and Hirt fatigue model

1. Introduction

Many constant amplitude loading fatigue crack growth models, such as the Paris[1] and the Walker and Forman models,[2] involve a number of empirical curve fitting parameters that have no physical basis. The only major differences among these models are the particular curve fitting technique used to fit the model to experimental fatigue rate data and the number of parameters they require. The main disadvantage of these models is that they are material dependent, which require calibrations of the empirical parameters from the fatigue testing of each different material. Fatigue testing is expensive and time consuming; therefore, it is desirable to use fatigue models that have some physical significance by using known material properties determined from less lengthy tests. One such attempt to create a fatigue crack growth model based on physical significance resulted in the Zheng and Hirt model,[3,4] which does not involve fatigue testing to establish the empirical parameters as required by the aforementioned models. Instead, the Zheng and Hirt model relies on the tensile properties and the fatigue crack growth threshold value, thus making it a cost-effective fatigue crack propagation methodology. The Zheng and Hirt model is moderately successful in predicting fatigue crack growth rates and this report presents a proposed modification to the model to improve its accuracy in predicting fatigue crack growth rates.

2. Background

2.1 Description of Zheng and Hirt Model

The Zheng and Hirt model is a constant-amplitude, loading fatigue model originally developed for metals. It is a modification of the static fracture model proposed by Lal and Weiss,[5] which assumes that the crack growth per loading cycle is equal to the distance in which the maximum normal stress σ is greater than the critical fracture stress σ_{ff} of the metal, as shown in Fig. 1. From this assumption, the following equation can be derived from linear elastic fracture mechanics:

$$\frac{da}{dN} = B\Delta K_{eff}^2 = \frac{1}{2\pi\sigma_{ff}^2}(\Delta K - \Delta K_{th})^2, \quad \text{(Eq 1)}$$

where da/dN is the crack growth per cycle, ΔK is the applied stress intensity factor range and ΔK_{th} is the fatigue crack growth threshold. The critical fracture stress σ_{ff} is in turn taken as the theoretical strength of metallic materials:

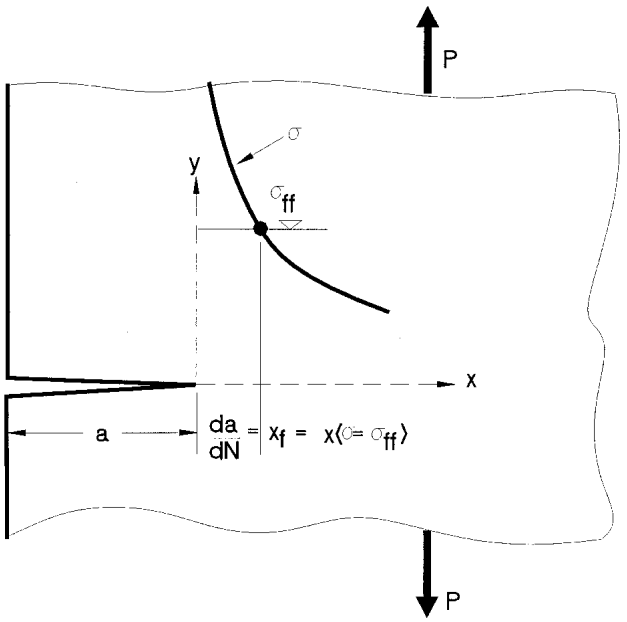

Fig. 1 Schematic illustration of the assumption of the amount of incremental fatigue crack propagation[3]

B.K.C. Yuen and **F. Taheri,** Department of Civil Engineering, Dalhousie University, 1360 Barrington Street, Halifax, Nova Scotia, B3J 1Z1, Canada. Contact e-mail: farid.taheri@dal.ca.

Table 1 Tensile Properties and Reanalyzed Results for Various Steels

Material	σ_u, MPa	σ_y, MPa	RA, %	R	B, MPa^{-2} Reanalyzed	B, MPa^{-2} Predicted	ΔK_{th}, MPa $m^{1/2}$	$B_{Predicted}/B_{Reanalyzed}$
Martensite steels								
18Ni(900)	1769	1679	31.0	0.05-0.2	8.67×10^{-10}	9.29×10^{-10}	11.15	1.07
18Ni(1100)	1587	1493	35.6	0.05-0.2	8.37×10^{-10}	8.50×10^{-10}	7.76	1.02
4340(200)	2324	1325	17.2	0.05-0.2	1.97×10^{-8}	1.55×10^{-9}	19.90	0.08
4340(500)	1714	1521	26.3	0.05-0.2	1.37×10^{-9}	1.36×10^{-9}	14.05	0.99
H-11	1958	1424	31.8	0.05-0.2	1.37×10^{-8}	9.10×10^{-10}	19.86	0.07
D6AC	1618	1499	36.5	0.1-0.3	4.53×10^{-10}	7.73×10^{-10}	6.78	1.71
12Ni-5Cr-3MO	1290	1269	64.0	0-0.7	2.72×10^{-10}	3.70×10^{-10}	2.73	1.36
H-130	1015	936	70.0	0-0.7	3.14×10^{-10}	3.70×10^{-10}	2.24	1.18
10Ni-Cr-Mo-Co	1434	1310	72.0	0-0.7	2.11×10^{-10}	2.47×10^{-10}	8.53	1.17
9Ni-4Co-0.25C	1338	1257	61.0	−0.1-0.25	4.10×10^{-9}	3.87×10^{-10}	27.86	0.09
10Ni-8Co-Mo	951	917	69.0	…	3.06×10^{-10}	4.11×10^{-10}	4.65	1.34
30CrMnSiNi2	1676	1387	45.0	0.2	7.42×10^{-10}	5.59×10^{-10}	2.26	0.75
Pearlite-ferrite steels								
A357A	569	405	73.0	0-0.7	5.38×10^{-10}	5.99×10^{-10}	10.17	1.11
A302B	604	384	67.0	0-0.7	4.27×10^{-10}	6.93×10^{-10}	11.37	1.62
A36	514	247	68.0	0-0.7	3.59×10^{-10}	7.84×10^{-10}	10.06	2.18
ABS-C	432	268	66.0	0-0.7	3.21×10^{-10}	9.98×10^{-10}	9.62	3.11
SAE0030	494	302	46.0	0	7.54×10^{-10}	1.74×10^{-9}	17.60	2.31
				−1	5.95×10^{-10}	1.74×10^{-9}	20.01	2.92
SAE1020	412	261	58.0	0	1.48×10^{-9}	1.37×10^{-9}	24.71	0.93
				−1	1.68×10^{-9}	1.37×10^{-9}	21.00	0.82
A572	535	370		0	5.95×10^{-10}	8.92×10^{-10}	20.01	1.50
				−1	9.09×10^{-10}	8.92×10^{-10}	20.88	0.98
Quenched-tempered steels								
4340(1000)	1205	1120	38.8	0.05-0.2	9.03×10^{-10}	9.46×10^{-10}	13.28	1.05
4340(1400)	665	431	53.3	0.05-0.2	1.64×10^{-9}	9.97×10^{-10}	21.00	0.61
AISI403(Heat637)	769	641	56.5	…	2.61×10^{-10}	7.65×10^{-10}	6.45	2.93
AISI403(Heat933)	748	611	53.1	…	4.23×10^{-10}	8.92×10^{-10}	8.31	2.11
AISI403(Heat484)	817	678	48.5	…	2.23×10^{-10}	9.60×10^{-10}	7.43	4.30
5Ni-Cr-Mo-V	1043	974	68.0	0.1	2.30×10^{-10}	3.87×10^{-10}	5.79	1.68
SAE4140(720)	1468	1372	55.0	0	1.25×10^{-10}	4.25×10^{-10}	−4.48	3.40
				−1	1.43×10^{-10}	4.25×10^{-10}	−1.20	2.97
SAE4140(970)	1146	1098	59.0	0	1.32×10^{-10}	4.72×10^{-10}	5.79	3.58
				−1	2.95×10^{-10}	4.72×10^{-10}	9.40	1.60
SAE4140(1230)	720	617	63.0	0	2.07×10^{-10}	6.63×10^{-10}	13.23	3.20
				−1	2.66×10^{-10}	6.63×10^{-10}	11.59	2.49

$$\sigma_{ff} = \sqrt{E\sigma_f\varepsilon_f}, \quad \text{(Eq 2)}$$

where E is the modulus of elasticity, and σ_f and ε_f are the material's fracture strength and fracture ductility, respectively. The true fracture strength and fracture ductility are given in Ref. 6 as

$$\sigma_f = \sigma_u (1 + RA) \quad \text{(Eq 3)}$$

$$\varepsilon_f = -\ln(1 - RA) \quad \text{(Eq 4)}$$

where σ_u is the ultimate stress and RA is the reduction in area at fracture in a tension test.

2.2 Reanalysis of Existing Test Data

To illustrate the rationale for modifying the Zheng and Hirt model, the fatigue crack propagation test data for various steels was reanalyzed in Ref. 3 to compare the predicted values of constant B from tensile properties and the reanalyzed values. The reanalysis involved taking the logarithmic transformation of Eq 1 to obtain:

$$\log \frac{da}{dN} = \log B + 2\log(\Delta K - \Delta K_{th}) \quad \text{(Eq 5)}$$

which represents a straight line with a slope of 2 when $\log(da/dN)$ is plotted against $\log(\Delta K - \Delta K_{th})$. The values of B and ΔK_{th} were obtained by trial and error such that the slope was approximately 2 through a linear regression analysis. The results of the reanalysis are shown in Table 1. It can be seen that Eq 1 over-predicted the value of B in most cases. In fact, the ratio of the predicted value of B to the reanalyzed value of B ranged from 0.07 to 4.30.

2.3 Proposed Modification to the Model

In the Zheng and Hirt model, the fracture strength of the material is calculated based on the ultimate strength of the material (Eq 3). However, it is debatable whether the ultimate strength, defined as the maximum nominal stress attained in a

conventional tension test, can be related to the stress at fracture. Instead, it is proposed that the fracture strength of the material should be obtained from the measured true stress at fracture in a tension test, that is, the final fracture load divided by the final fracture area. It is therefore postulated that using such measured fracture strength of material should provide a better-predicted value of B in Eq 1.

To verify the above hypothesis, an experimental investigation was performed on samples of steel. The investigation consisted of performing tension tests to obtain the tensile properties of 350WT steel, a constant amplitude loading fatigue test to provide baseline fatigue data, a fatigue crack growth threshold test to determine the threshold value and a reanalysis of the baseline fatigue data to compare the predicted values of B from using Eq 3 and from the measured true fracture strength of the steel. The 350WT steel described in these papers is widely used in Canadian navy frigates and for bridges. The following sections describe the fatigue testing procedure and discuss the results of the tests.

3. Experimental Procedure

3.1 Overview

The experimental fatigue crack propagation testing consisted of subjecting center-cracked specimens of 350WT steel to a constant-amplitude loading test and a fatigue crack growth threshold test. All fatigue crack growth tests were conducted in accordance with ASTM Standard E 647, Standard Test Method for Measurement of Fatigue Crack growth Rates.[7] The test method covers the determination of fatigue crack growth rates from fatigue testing, including discussions on special requirements for various specimen configurations and recommended techniques from calculating the fatigue crack growth rates.

3.2 Test Material

The material used in this investigation was 350WT category 5 steel provided by Defense Research and Development Canada-Atlantic. This type of steel is both weldable and notch tough at low temperature, with a minimum required yield strength of 350 MPa and a Charpy V-Notch toughness of at least 40 J at –40 °C. It is a typical material used in the hull of Halifax class frigate as well as bridges, pressure vessels and offshore structures. The chemical composition of the steel is presented in Table 2.

Three tension tests were performed on the steel in accordance with ASTM E 8M, Standard Test Methods for Tension Testing of Metallic Materials[8] to provide the required tensile properties for the Zheng and Hirt fatigue model. The average results of the tension tests are shown in Table 3. It can be seen that the measured true fracture strength (1063 MPa) is significantly higher than the fracture strength (836 MPa) calculated from Eq 3.

3.3 Fatigue Test Specimen

The test specimens used in the fatigue investigation were rectangular specimens with a center-crack, as shown in Fig. 2. Similar specimens were used to characterize the threshold and

Table 2 Chemical Composition of 350WT Steel

Specimen, %	Element	350WT, %
0.075	Carbon	0.22 max
0.034	Chromium	…
0.016	Cobalt	…
0.010	Copper	…
1.250	Manganese	0.80-1.50
0.006	Molybdenum	…
0.300	Niobium	…
0.008	Nickel	…
0.009	Phosphorus	0.03 max
0.230	Silicon	0.15-0.40
0.052	Vanadium	…
0.004	Sulphur	0.03 max

Table 3 Material Properties of 350WT Steel

Material Property	Value
Yield Stress, σ_{yld}	365 MPa
Ultimate Stress, σ_{ult}	496 MPa
Reduction in Area, RA	68%
Modulus of Elasticity, E	200 GPa
Poisson's Ratio, ν	0.3(a)
Fracture Strength, σ_f	1.063(b)/836(c) MPa
Fracture Ductility, ε_f	1.15(d)

(a) From Ref. 8
(b) Determined experimentally
(c) Eq 3
(d) Eq 4

response of the material under variable amplitude testing.[9,10] ASTM E 647 provides recommended dimensions and equations for calculating the stress intensity factor for such a specimen. The test specimen layout and dimensions are shown in Fig. 2. The specimens were cut lengthwise in the rolling direction of the steel such that the fatigue cracks would grow traverse to the rolling direction. Seven grip holes of approximately 11 mm (7/16 in.) diameter were drilled at each ends of each specimen to accommodate the grips of the test fixture. A small hole of 3.2 mm (1/8 in.) diameter was drilled at the center of the specimen to allow a starter notch to be machined from each side of the hole. The starter notch for each specimen was done at the Halifax Dockyard machine shop (Halifax, Nova Scotia) by the electrical discharge machining process, resulting in a notch width of 0.254 mm (0.010 in.). The specimen's surface was then polished to provide a clear image of the crack tip when observed under a microscope. In summary, the overall specimen dimensions were approximately 300 × 100 × 6.35 mm (1/4 in.), with a starter notch length (2a) of approximately 20 mm.

3.4 Test Apparatus

An Instron model 8501 (Canton, MA) servo-hydraulic universal testing machine was used to perform the fatigue testing. The machine used an Instron digital control panel (model 8500+) and a load cell with a capacity of ±100 and 200 kN under dynamic and static loading conditions, respectively. Each of the test specimens was mounted to the machine by the

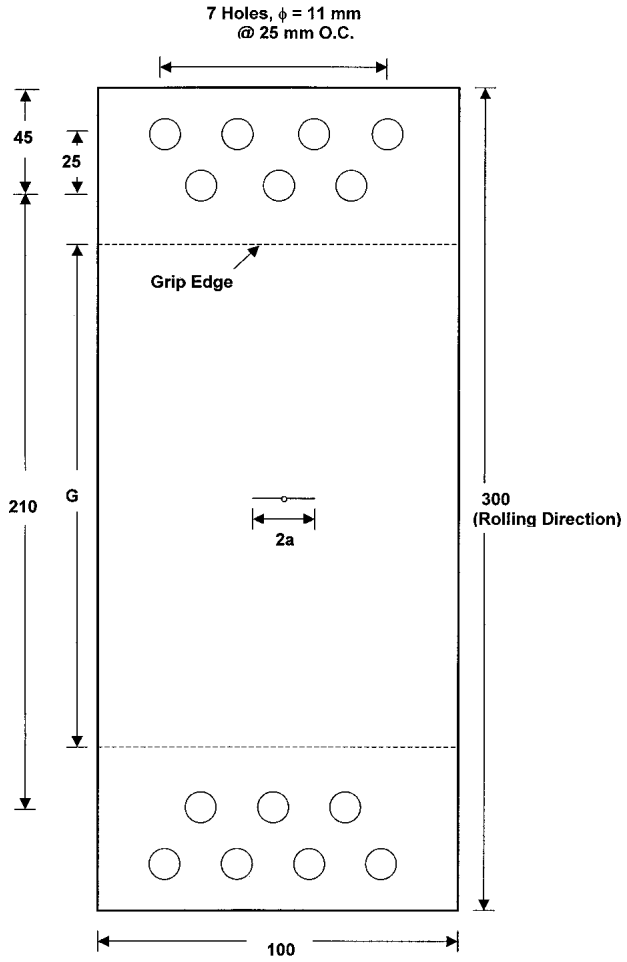

Fig. 2 Specimen layout and dimensions

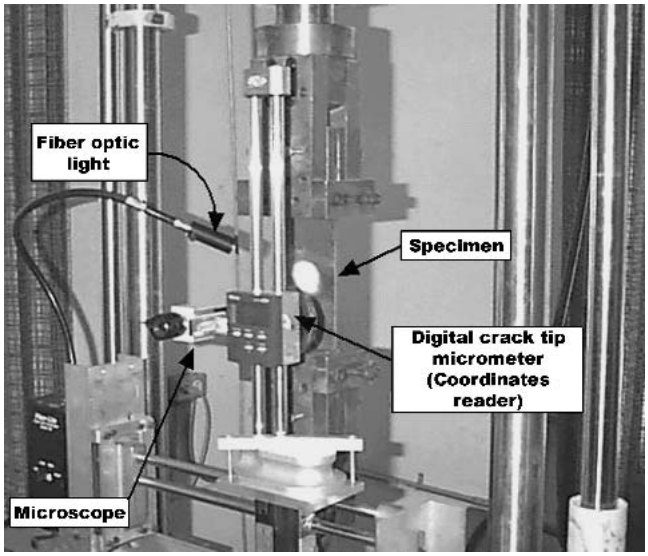

Fig. 3 Completely assembled experimental setup

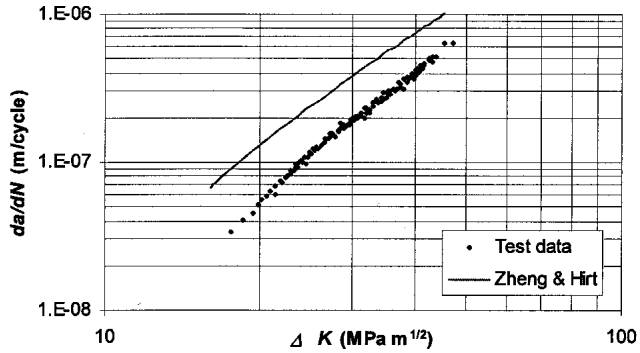

Fig. 4 Fatigue rate curves from constant amplitude loading test and from Zheng and Hirt prediction

way of grips and fixtures, which were screwed into the load cell at the top and the actuator at the bottom. A traveling microscope consisting of a microscope at 10× magnification attached to two micrometers with resolutions of 0.01 mm were used to measure incremental fatigue crack growth. Finally, a fiber optic light was used to illuminate the crack tip region. The completely assembled experimental setup is shown in Fig. 3.

3.5 Test Procedure

All fatigue tests were performed in accordance with ASTM E 647. The fatigue loading on the specimens comprised of axial tension in a sinusoidal waveform at room temperature in air. In all cases, the baseline constant amplitude loading consisted of cycles at maximum load of 60 kN and stress ratio R (ratio of minimum load P_{min} to maximum load P_{max}) of 0.1 at a load frequency of 20 Hz. All the specimens were precracked to a minimum length of 1.0 mm on both sides of the starter notch as required by the standard before valid crack length data was recorded. This procedure removed the effect of the blunt starter notch and provided a sharpened fatigue crack of adequate size and straightness. For each specimen, the crack length was measured by a traveling microscope at specific number of elapsed cycles, such that the crack growth between measurements would be less than 1 mm whenever possible. For all specimens, the crack length data was calculated by the average of the left and right cracks and reduced to fatigue crack growth rate data by the secant and the incremental methods as recommended by ASTM E 647.

4. Experimental Results and Discussion

4.1 Constant Amplitude Loading Test Results

The constant amplitude-loading test involved testing a number of specimens at the baseline constant amplitude loading described above until failure. The average results are presented by plotting the crack growth rate (ΔK) against the corresponding stress intensity factor range (da/dN), or fatigue rate curve, in Fig. 4. The Paris equation for this type of steel was given by

$$\frac{da}{dN} = 1.11 \times 10^{-11} (\Delta K)^{2.86}, \quad \text{(Eq 6)}$$

where da/dN is in m/cycle and ΔK is in MPa m$^{1/2}$.

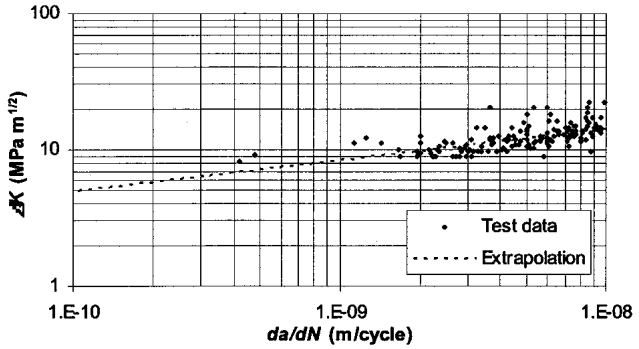

Fig. 5 Fatigue crack growth threshold test results and extrapolation

4.2 Fatigue Crack Growth Threshold Test Results

The fatigue crack growth threshold test involved testing a number of specimens at constant amplitude loading but reducing the maximum load by 10% in successive steps while keeping the stress ratio at 0.1 until fatigue crack growth rates between 10^{-9} and 10^{-10} m/cycle were achieved. The operational fatigue crack growth threshold (ΔK_{th}), as defined in the ASTM E 647, was then obtained by linearly extrapolating the fatigue crack growth data to a fatigue crack growth rate of 10^{-10} m/cycle on a log-log graph as shown in Fig. 5. A value of ΔK_{th} = 5.76 MPa $m^{1/2}$ was obtained in the current study, which compared well with the value of 6.00 suggested by Barsom and Rolfe.[11]

4.3 Fatigue Crack Growth Prediction by the Modified Zheng and Hirt Model

From the data obtained through our experimental investigation, the tensile properties and the fatigue crack growth threshold were determined for the 350WT steel. The modified Zheng and Hirt model for the steel could then be represented by

$$\frac{da}{dN} = 6.47 \times 10^{-10} (\Delta K - 5.76)^2, \quad \text{(Eq 7)}$$

where da/dN is in m/cycle and ΔK is in MPa $m^{1/2}$. The equation is plotted along with the constant amplitude loading test data in Fig. 4. It can be seen that the model over predicted the fatigue crack growth rates of the specimen considerably, and thus would give a conservative estimate of its fatigue life.

A reanalysis similar to that of Ref. 3 was then performed to obtain the best-fit values of B and ΔK_{th} to our test data. By taking the square root of Eq 1, it becomes

$$\sqrt{\frac{da}{dN}} = \sqrt{B}\Delta K - \sqrt{B}\Delta K_{th}, \quad \text{(Eq 8)}$$

which represents a straight line with slope $\sqrt{B}$ when $\sqrt{da/dN}$ versus ΔK is plotted. Thus, a linear regression analysis would give the best-fit values of B and ΔK_{th} to the test data. Such reanalysis of our test data yielded the following equation:

$$\frac{da}{dN} = 4.17 \times 10^{-10} (\Delta K - 8.64)^2. \quad \text{(Eq 9)}$$

It can be seen that the reanalyzed value of ΔK_{th} was similar to that determined experimentally, and the ratio of the predicted value of B from tensile properties to the reanalyzed value of B was 1.55, which was within the range calculated from the reanalyzed data of Ref 3. Note that had Eq 3 was used to calculate the fracture strength of the steel instead, the predicted value of B would have been 8.23×10^{-10}, which would have over-predicted the actual fatigue crack growth rates even more so. Therefore, although both methods of calculating the fracture strength of the steel resulted in over predicting its fatigue crack growth rates, using the measured fracture strength was shown to provide a better prediction than using Eq 3 to calculate the fracture strength.

Finally, it is proposed that a different definition of the critical fracture stress σ_{ff} from the conventional tensile properties of the material, or perhaps the development of a new experimental technique for determining such critical fracture stress might further improve the accuracy of the predicted value of B.

5. Conclusion

A modification was proposed to the Zheng and Hirt constant amplitude fatigue model, using the measured fracture strength of the metal instead of the calculated strength. Standard tension tests were performed to determine the tensile properties, in particular the true stress at fracture of 350WT category 5 steel. A number of constant amplitude loading fatigue tests was performed on the steel to provide comparison to prediction, and fatigue crack growth threshold tests were performed to determine the necessary model parameter. Based on the analysis of tests results, it is concluded that the proposed modified Zheng and Hirt model using the measured fracture strength of the metal provides a better estimate of its fatigue crack propagation rates.

Acknowledgment

The financial support of NSERC and Defense Research Development Canada—Atlantic is gratefully acknowledged.

References

1. P.C. Paris and F. Erdogan: "A Critical Analysis of Crack Propagation Laws," *J. Basic Eng., Trans. ASME*, 1963, *85*, pp. 528-34.
2. N.E. Dowling, *Mechanical Behavior of Materials: Engineering Methods for Deformation, Fracture, and Fatigue*, Prentice Hall, Englewood Cliffs, NJ, 1993.
3. X. Zheng and M.A. Hirt: "Fatigue Crack Propagation in Steels," *Eng. Fract. Mech.*, 1983, *18*(5), pp. 965-73.
4. X. Zheng: "A Simple Formula for Fatigue Crack Propagation and a New Method for the Determination of ΔK_{th}," *Eng. Fract. Mech.*, 1987, *27*(4), pp. 465-75.
5. D.N. Lal and V. Weiss: "A Notch Analysis of Fracture Approach to Fatigue Crack Propagation," *Metall. Trans.*, 1978, *9*(A), pp. 413-26.

6. X. Zheng: "Local Strain Range and Fatigue Crack Initiation Life," *IABSE Proc. Fatigue Colloq.*, 1982, pp. 169-78.
7. Anon: "ASTM Designation E 647-00," in *2000 Annual Book of ASTM Standards*, ASTM, West Conshohocken, PA, 2000, pp. 594-629.
8. Anon: "ASTM Designation E 8M-01," in *2001 Annual Book of ASTM Standards*, ASTM, West Conshohocken, PA, 2001, pp. 82-103.
9. P.A. Rushton, F. Taheri, and D.C. Stredulinsky: "Threshold and Variable Amplitude Crack Growth Behavior in 350WT Steel," *Proc. 21st Int. Conf. on Pressure Vessels and Piping, ASME-PVP*, 2002, *441*, pp. 81-89.
10. P.A. Rushton and F. Taheri: "Prediction of Variable Amplitude Crack Growth in 350WT Steel Using a Modified Wheeler Approach," *J. Marine Struct.*, 2003, *16*(7), pp. 517-39.
11. J.M. Barsom and S.T. Rolfe: *Fracture and Fatigue Control in Structures: Applications of Fracture Mechanics*, 3rd ed., ASTM, West Conshohocken, Pa, 1999.